Improved detection of preeruptive seismic velocity drops at the Piton de La Fournaise volcano

Diane Rivet, Florent Brenguier, Frédéric Cappa

AGU PUBLICATIONS

Geophysical Research Letters

RESEARCH LETTER
10.1002/2015GL064835

Key Points:
- Rainfall produces significant seismic velocity changes at Piton de la Fournaise volcano
- We correct seismic velocity change time series for pore pressure change effects
- After correction we identified a preeruptive velocity drop that was undetected

Supporting Information:
- Figure S2
- Figure S3
- Text S1

Correspondence to:
D. Rivet,
diane.rivet@geoazur.unice.fr

Citation:
Rivet, D., F. Brenguier, and F. Cappa (2015), Improved detection of preeruptive seismic velocity drops at the Piton de La Fournaise volcano, *Geophys. Res. Lett.*, *42*, 6332–6339, doi:10.1002/2015GL064835.

Received 5 JUN 2015
Accepted 24 JUL 2015
Accepted article online 29 JUL 2015
Published online 15 AUG 2015

Improved detection of preeruptive seismic velocity drops at the Piton de La Fournaise volcano

Diane Rivet[1], Florent Brenguier[2], and Frédéric Cappa[1,3]

[1]Géoazur, Université Nice Sophia Antipolis, Campus Azur, Sophia-Antipolis, France, [2]Institut des Sciences de la Terre, Université Joseph Fourier, Grenoble, France, [3]Institut Universitaire de France, Paris, France

Abstract The unexpected 2014 and 2015 Ontake (Japan) and Calbuco (Chile) eruptions proved that improving volcanic eruption prediction is still a great challenge. Decreases of seismic velocities of the Piton de la Fournaise volcano inferred from seismic noise correlations have been shown to precede eruptions. However, seismic velocities are strongly influenced by rainfall and subsequent pore pressure perturbations. Here we increase the detection of precursory seismic velocity changes to an eruption by removing the effects of pore pressure changes. During 2011–2013, the volcano exhibits a low eruptive activity during which we observe seismic velocity variations well correlated with rainfall episodes. We estimated the transfer function between fluid pressure and seismic velocity changes. We use these results to correct seismic velocity change time series for pore pressure changes, due to rainfall and found a preeruptive velocity drop (0.15%) associated with the 21 June 2014 eruption that was undetected before correction.

1. Introduction

Volcanic eruptions are sudden and short episodes in the history of volcanoes. Detecting precursory signals related to the magma ascent is a key issue to forecast volcanic eruption. Seismic velocity change monitoring using cross correlation of ambient noise is a powerful tool to detect eruption precursory signals that are characterized by a decrease of seismic velocity on the order of 0.1% for some days preceding the eruption [*Brenguier et al*., 2008a]. *Brenguier et al.* [2011] shown that intrusions that did not evolve into eruptions could be at the origin of some short-term velocity decreases. These velocity decreases are likely to result from magmatic activity interacting with the edifice (fluid pressurization, edifice damage, and deformation). The same way seismic velocity is sensitive to magmatic pressurization, it is sensitive to pore pressure changes produced by environmental effects. The duration and the amplitude of such seismic velocity change can be very similar to eruptive precursory signals. It is critical to correct seismic velocity changes related to environmental effects such as rainfall, to better detect seismic velocity changes related to intrusion and precursory magmatic movement before volcanic eruptions.

Coupling between atmospheric perturbations and solid Earth has been proposed to be responsible for the triggering and modulation of a series of geological phenomena. Correlations of crustal earthquakes and meteorological events have been observed numerous times and are referred to as hydroseismicity (see *Costain and Bollinger* [2010] for a review). Rainfalls also trigger slope instabilities [*Husen et al*., 2007; *Helmstetter and Garambois*, 2010; *Cappa et al*., 2014], and deep slow earthquakes can be triggered by large typhoons [*Liu et al*., 2009]. Put together, these observations provide strong evidence that hydromechanical coupling impact largely geological phenomenon. In several contexts fluid pressure diffusion is responsible of such hydromechanical interaction: reservoir-induced seismicity [*Talwani*, 1997], fluid injections in wells [*Zoback and Harjes*, 1997; *Shapiro et al*., 2003; *Fischer et al*., 2008; *Derode et al*., 2015], and rainfall-induced seismicity [*Muco*, 1995; *Hainzl et al*., 2006, 2013; *Kraft et al*., 2006; *Svejdar et al*., 2011].

Among other applications, seismic noise monitoring is used to quantify fluctuations of crustal properties associated with volcanic activity [*Brenguier et al*., 2008a, 2008b; *Obermann et al*., 2013] and long-term dynamics [*Sens-Schönfelder et al*., 2014; *Rivet et al*., 2014]. However, there are evidences that rainfall and the water level changes affect seismic wave velocities [*Sens-Schönfelder and Wegler*, 2006; *Meier et al*., 2010; *Tsai*, 2011; *Froment et al*., 2013; *Hillers et al*., 2014; *Gassenmeier et al*., 2015] and produce seismic velocity changes of the same order of amplitude than those produced by the investigated geological process.

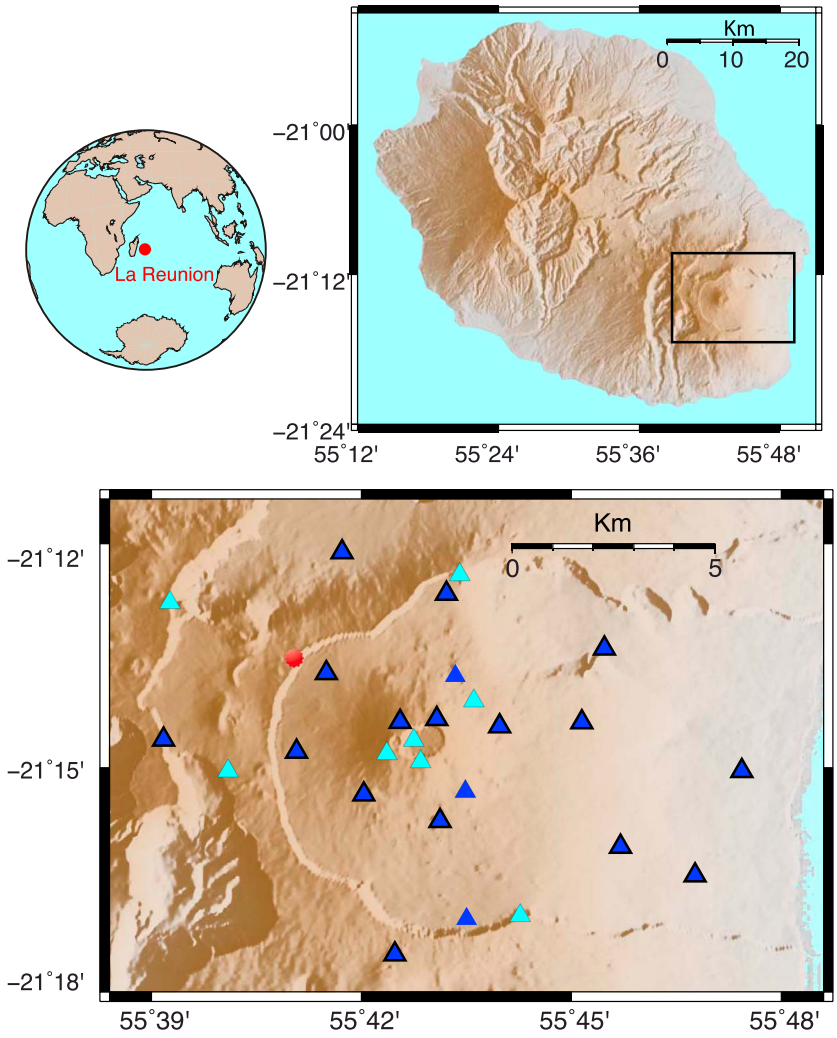

Figure 1. Maps of the PdF volcano on the La Réunion Island in the Indian Ocean. The blue and cyan triangles indicate the broadband and short-period seismic stations, respectively, used to measure the seismic velocity change from June 2009 to December 2014. The triangles with black contour show the sites that were reequipped after Undervolc campaign. The red dot indicates the position of the Meteo France meteorological station Bellecombe on the eastern border of the Enclos Fouqué caldera rim.

Here we measure seismic velocity changes at the Piton de la Fournaise (PdF) volcano using cross correlations of ambient seismic noise recorded by a dense network of 27 stations between June 2009 and December 2014. The PdF volcano located on La Reunion Island, in the Indian Ocean, is a very active volcano with on average two eruptions per year (Figure 1) [*Roult et al.*, 2012; *Peltier et al.*, 2009]. The time period following the massive eruption of April 2007 is characterized by long-term summit deflation [*Rivet et al.*, 2014; *Peltier et al.*, 2015] associated with long-term velocity increase [*Rivet et al.*, 2014] and lower volcanic activity [*Roult et al.*, 2012]. During this quiet period we observe a correlation between velocity changes and rainfall. We estimate the fluid pressure change at depth produced by the rainfall using a fluid pressure diffusion formulation proposed by *Talwani et al.* [2007]. Between January and December 2013, a period with no eruption, we built a transfer function between the fluid pressure and the seismic velocity changes. We then estimate the synthetic velocity change produced by rainfall between June 2009 and December 2014 based on the transfer function. Finally, we correct the observed velocity changes for the synthetic velocity change to improve the detection of perturbation related to the PdF magmatic activity. As a result of this correction, we show a pre-eruptive velocity drop of 0.15% of the 21 June 2014 eruption that was undetected before in the original, uncorrected data.

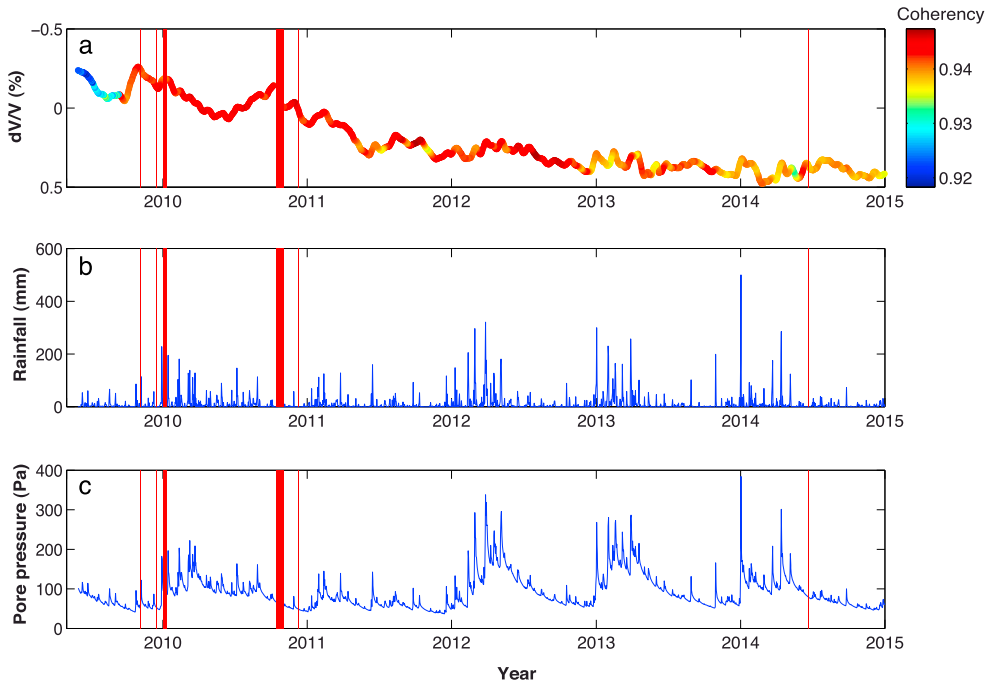

Figure 2. (a) Relative seismic velocity change time series of the PdF volcano. The color of the velocity change dots indicates the coherency between the reference and 8 day cross-correlation functions. The vertical red bars mark the periods of eruptive activity. (b) Daily rainfall measured at Bellecombe meteorological station located on the western edge of the Enclos Fouque. (c) Average fluid pressure change between the free surface and 6 km depth produced by the rainfall and computed from a diffusive model proposed by *Talwani et al.* [2007] and *Roeloffs* [1988].

2. Data and Method

2.1. Seismic Noise Cross Correlation and Velocity Change Measurements

We use seismic noise continuously recorded by the monitoring network of PdF volcano from June 2009 to December 2014. From September 2009 to June 2011, a high-resolution seismic network ("*UnderVolc*" experiment [*Brenguier et al.*, 2012]) composed of 15 broadband stations has been deployed to complement the 6 broadband stations of the permanent observatory. Afterward, many sites were reequipped, and until December 2014, we use records of 19 broadband sensors and 8 short-period sensors (Figure 1).

Seismic noise cross correlations and seismic velocity changes are processed the same way as in *Rivet et al.* [2014] and *Mordret et al.* [2014]. Continuous seismic records are band-pass filtered between 0.25 and 2 Hz, then sections of signal with amplitude greater than 10 times the standard deviation are discarded, and finally, we apply spectral whitening and 1-bit normalization. Seismic noise cross correlations are computed between pairs of stations for the vertical components over a moving 8 day window shifted everyday. We then measure seismic velocity change from the time delays between a reference cross correlation averaged over the entire period and the 8 day cross-correlation functions. Considering a homogeneous change of the seismic velocity in the medium, the relative difference in travel time is related to the relative change in the seismic velocity by $dt/t = -dv/v$. The relative travel time change is then measured in the frequency domain using the Multiple Window Cross-Spectral Analysis method initially proposed by *Poupinet et al.* [1984]. We estimate the reliability of the measurements from both the coherency between the reference and 8 day cross correlations (Figure 2a) and the error of the linear regression in time domain to measure dt/t [*Poupinet et al.*, 1984; *Clarke et al.*, 2011]. Finally, to better observe the average behavior of the PdF, we average seismic velocity changes over all station pairs.

2.2. Rainfall-Induced Fluid Pressure Changes

From reservoir-induced seismicity, *Talwani et al.* [2007] proposed a formulation of the poroelastic response of the first kilometers of the crust to the reservoir impoundment and lake level fluctuations. Two different responses produce changes in strength and induce seismicity. The first one is instantaneous and corresponds to the undrained response to loading [*Skempton*, 1954]. The second one is a delayed response due to the

diffusion of fluid pressure. This response involves both the increase in fluid pressure by diffusion from the surface to depth and the decrease in fluid pressure by relaxation (i.e., diffusion outside the system). The hydrologic property controlling fluid pressure diffusion is the hydraulic diffusivity (ratio of permeability to storativity). In most cases of induced seismicity, seismicity migration seems to be driven by the diffusion of fluid pressure [*Talwani*, 1997; *Chen and Talwani*, 2001]. These results suggest that fluid pressure during rainfall episodes could also impact the mechanical properties and therefore seismic velocities at depth.

Based on the observation of 90 case histories of induced seismicity, *Talwani et al.* [2007] validated the formulation of *Roeloffs* [1988] for the poroelastic response of rocks to a change in water level. In the *Roeloffs*'s [1988] formulation, all fractures are considered as fluid filled and only fluid pressures confined to the fractures are considered. The solution for a one-dimensional fully coupled diffusion equation gives the fluid pressure at a distance r, at a time t, as

$$p(r,t) = \alpha p_0 erf\left[\frac{r}{(4ct)^{1/2}}\right] + p_0 erfc\left[\frac{r}{(4ct)^{1/2}}\right], \quad (1)$$

where $p(0,t) = p_0$, $p_0 = 0$ for $t < 0$ and $p_0 = 1$ for $t < 0$; *erf* is the error function and $erfc = 1 - erf$; c is the hydraulic diffusivity; and $\alpha = B(1+\nu_u)/3(1-\nu_u)$ is an elastic constant linked to the Skempton's coefficient B and the undrained Poisson ratio ν_u. The first term of equation (1) describes the undrained response of the medium with rapid pressure increase at time $t = 0$ due to the elastic effect and its poroelastic relaxation, while the second term characterizes the fluid pressure at a distance from an applied load at the surface due to diffusion.

In a fully saturated poroelastic medium, the fluid pressure changes at depth associated with the groundwater level change depend on the rainfall history and the hydraulic properties. We consider a simple model where the groundwater level change is equal to the deviation of the rainfall from the average precipitation rate. Other model exists, but *Hainzl et al.* [2013] and *Niu et al.* [2007] found that the fluid pressure results are not strongly dependent on the groundwater model. A time-varying groundwater load change can be numerically regarded as a succession of load changes. Hence, the fluid pressure can be deduced by superposing the effects of each load change expressed by equation (1) [*Talwani et al.*, 2007]:

$$P_i(r,t) = \sum_{i=1}^{n} \alpha \delta p_i erf\left[\frac{r}{(4c(n-i)\delta t)^{1/2}}\right] + \sum_{i=1}^{n} \delta p_i erfc\left[\frac{r}{(4c(n-i)\delta t)^{1/2}}\right], \quad (2)$$

where n is the number of time increments δt between the start of the rainfall time series and the time t and δp_i is the groundwater load change variation at the sampled instant $t_i = i \times \delta t$ [10]. Here we assume that pore pressure diffusion is a possible mechanism for influencing seismic velocity changes in our study area. Because effects of rainfall-induced stress changes at depth are not well constrained due to the inherent difficulties in measuring poroelastic parameters at depth in high permeable rocks such as the ones studied here, we focus on the direct effect of pore pressure changes due to diffusion only. This pore pressure diffusion approach was previously used to study the potential links between rainfall and seismicity [*Hainzl et al.*, 2006; *Kraft et al.*, 2006; *Talwani et al.*, 2007] as well as seismic velocity changes [*Sens-Schönfelder and Wegler*, 2006; *Hillers et al.*, 2014]. We tested several values of hydraulic diffusivity c from 0.1 to 10 $m^2 s^{-1}$. In the following we fixed $c = 4$ $m^2 s^{-1}$ according to *Fontaine et al.* [2002] (see supporting information). Rainfall is measured at the Meteo France meteorological station "*Bellecombe*" located on the eastern border of the Enclos Fouque (Figure 1). Rainfall and the averaged fluid pressure change between the free surface and 6 km depth are shown in Figures 2b and 2c, respectively.

3. Results

3.1. Seismic Velocity Change Time Series

Between 2009 and the end of 2010, several eruptions occurred and produced seismic velocity changes with a decrease of velocity of less than 0.1% observed prior to the volcanic eruptions and followed by a recovery of the velocity [*Obermann et al.*, 2013]. From the beginning of 2011 to June 2014, there was no eruption and no evidence of intrusion or increase in seismic activity. However, the average seismic velocity of the volcano undergoes about 20 short-term perturbations, from 0.5 to 2 months long, with amplitude that can reach 0.1%. Finally, the volcano enters in eruption on 21 June 2014, after 3 years of no eruptive activity. The seismic velocity change produced by this eruption is of the order of previous fluctuations, and it is hardly detectable.

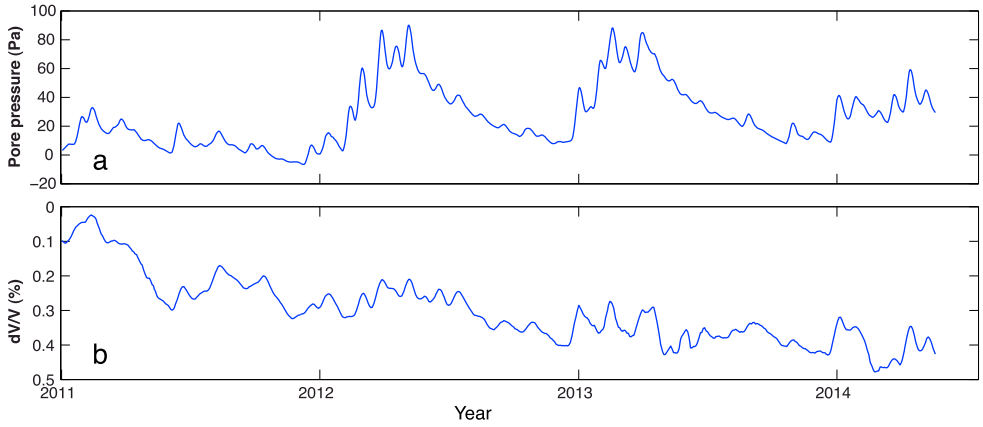

Figure 3. Comparison between (a) fluid pressure and (b) seismic velocity changes measured on an 8 day moving window during the quiet period with no eruptive activity, between January 2011 and May 2014.

In addition to short-term changes, the 5.5 year time series shows a long-term change with continuous increase of the velocity related to the deflation of the volcano after the major eruption of April 2007 [*Rivet et al.*, 2014].

In the following, we first investigate the origin of short-term velocity changes during the quiet period of 2011 to mid-2014, and, in particular, we explore the relationship between fluid pressure change due to rainfall and seismic velocity changes. Then, we estimate a transfer function between both variables while the volcano remains quiet. Because the mechanisms that are responsible for seismic velocity variations during a fluid pressure change are not well constrained, we choose to use a signal-processing approach by building a transfer function to better estimate the seismic velocity change induced by fluid pressure changes.

Figure 3 shows a comparison between the mean fluid pressure change estimated between the free surface and 6 km depth and the seismic velocity changes, from the beginning of 2011 to June 2014. We observe that short-term velocity decreases (i.e., 1–2 months long) are well correlated with increases in fluid pressure due to rainfall episodes. For longer-period variations than ~100 days, it is not clear how the fluid pressure affects the seismic velocity.

3.2. Synthetic Seismic Velocity Changes Produced by Fluid Pressure Change

In order to determine which period bands of the seismic velocity changes are affected by changes in fluid pressure, we band-pass filter in different period bands the fluid pressure and the velocity change time series, and we estimate the correlation coefficient R between both. Figure S2 in the supporting information presents a 2 year time series of both seismic velocity and fluid pressure changes filtered in five different bands: 300–120 days (Figure S2b), 120–60 days (Figure S2c), 60–30 days (Figure S2d), 30–16 days (Figure S2e), and 16–8 days (Figure S2f). Seismic velocity and fluid pressure changes are well correlated for the bands 60–30 and 30–16 days, with a coefficient of correlation of 0.84 and 0.73, respectively. This observation suggests that the velocity changes, during this 2 year period, are mainly due to rainfall. For longer periods, the correlation coefficient decreases. This indicates either that long fluid pressure changes are less prone to induce seismic velocity changes or our model of fluid pressure change is evolving over time. At shorter period, between 16 and 8 days, no correlation is observed.

From January 2011 to December 2012, we estimate the transfer function between fluid pressure and seismic velocity changes (Figure 4a). The transfer function is a mathematical representation for fit between an input and an output, in our case between the fluid pressure change and the seismic velocity change, respectively. For each period band B_i for which we observe a correlation between both variables, we assume that seismic velocity change is proportional to fluid pressure: $dV/V(B_i) = K(B_i) \times P(B_i)$. Through a statistical approach we deduce that the covariance of both terms is proportional to the variance of the fluid pressure:

$$\mathrm{cov}\left(\frac{dV}{V}(B_i), P(B_i)\right) = K(B_i) \times \mathrm{var}(P(B_i)). \quad (3)$$

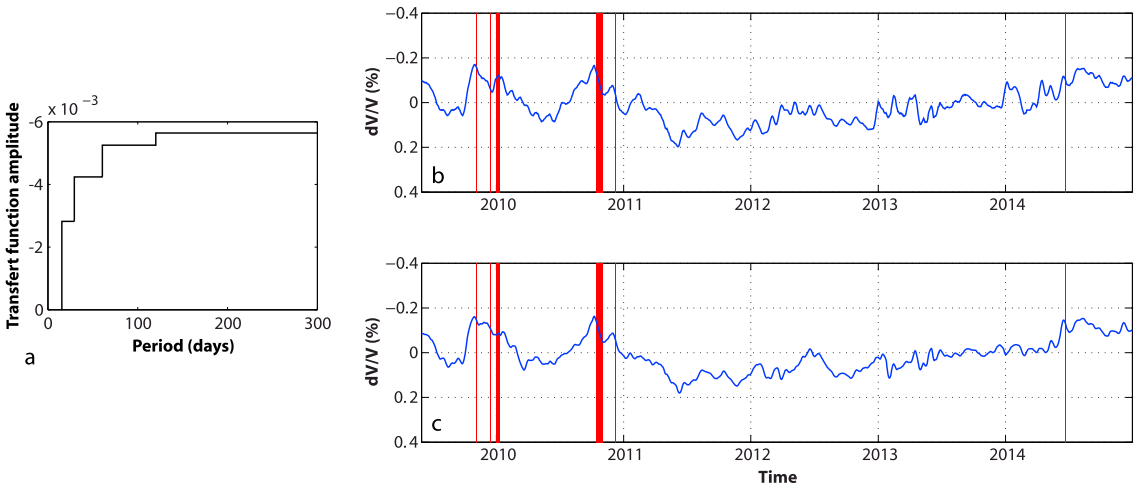

Figure 4. (a) Transfer function between fluid pressure and seismic velocity changes estimated from the 2011–2012 time series and seismic velocity changes measured at PdF volcano (b) without and (c) with a correction of rainfall effects. Note that on both time series the long-term trend of increasing velocity has been removed.

We then estimate the amplitude factor K for each period band with

$$K(B_i) = \frac{\mathrm{cov}\left(\frac{dV}{V}(B_i), P(B_i)\right)}{\mathrm{var}(P(B_i))} \tag{4}$$

and obtain the corresponding amplitude transfer function between the input and output. We assume no phase delay between the fluid pressure change and the seismic velocity change because the delay between rainfall and fluid pressure is already controlled by the hydraulic diffusivity c in the fluid pressure estimation, and no systematic phase shift was observed between fluid pressure and velocity change. We finally apply the transfer function to the fluid pressure and obtain a synthetic seismic velocity change time series produced by fluid pressure changes. Figure S3 presents the comparison between synthetic and observed seismic velocity changes band-pass filtered between 300 and 16 days for the quiet period between January 2011 and June 2014. The coefficient of correlation between both time series is 0.72, which suggests that most of the velocity changes during this time period can be explained by changes in fluid pressure due to rainfall.

3.3. Correcting Seismic Velocity Change Time Series From Rainfall Effects

We use the synthetic seismic velocity changes produced by fluid pressure changes during rainfalls to correct observed times series. We subtract from the initial 5.5 year time series the synthetic seismic velocity changes that account for fluid pressure change effects. Figure 4 shows the seismic velocity change time series detrended from the long-term increase of velocity, before (Figure 4b) and after (Figure 4c) removing seismic velocity changes due to rainfall. Between 2009 and 2010, seismic velocity changes associated with eruptions are conserved. However, we can observe, after correction of rainfall effects, that for the 14 October 2010 eruption the precursory decrease of velocity accelerates as it approaches the eruption. During the quiet period (i.e., no eruptive activity), the amplitude of fluctuations reduces by about 20%. This relative low reduction of fluctuations can arise from an incomplete

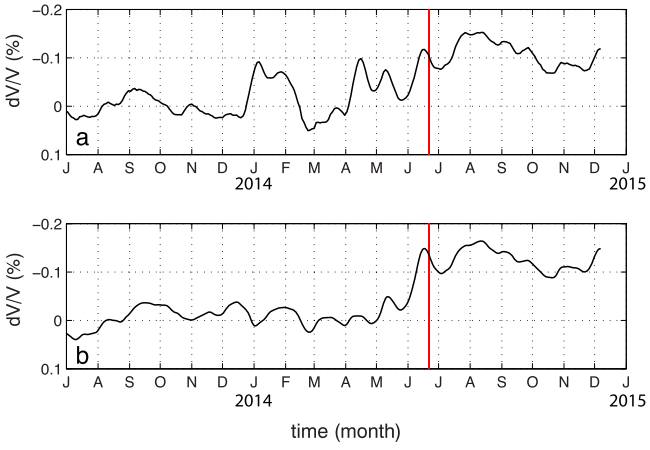

Figure 5. Close-up view of seismic velocity changes from July 2013 to December 2014 (a) without and (b) with rainfall effects corrected.

correction of meteorological effects or that after correction some random fluctuation and/or undetected velocity changes associated to deeper phenomena appear. Finally, the 21 June 2014 eruption was preceded by a seismic velocity decrease of ~0.1%, which is about the same amplitude as previous fluctuations observed months before (Figure 5a). After applying the correction of fluid pressure changes, the precursory signal appears clearly with a higher amplitude of −0.15%, while the other velocity decreases observed in 2014 were reduced. Consequently, with the correction of rainfall effects on the seismic velocity changes, it is possible to detect precursory signals that were undetected because of environmental fluctuations of the seismic velocity.

4. Conclusion

Thanks to seismic noise cross correlations corrected for fluid pressure effects, we identified a precursory signal with higher amplitude than ones conventionally estimated before eruptions at PdF volcano. Our interpretation suggests that seismic velocity changes are sensitive to fluid pressure diffusion. Transient decreases of seismic velocity produced by heavy rainfall reach 0.1% and are of the same order of magnitude than precursory velocity drop observed prior to the eruptions. We can assume that both increases in fluid pressure in the hydrothermal system due to rainfall and in the volcano feeding system preceding eruptions produce similar changes in the fractured rock of the volcano such as the opening of fractures. Therefore, similarly to the triggering of seismicity by change in fluid pressure frequently observed in various geological regions, we would expect that in certain condition strong rainfall may play a role in the triggering of eruptions.

The correction of rainfall effects from seismic velocity change measurements would be improved by a better spatial coverage of rainfall measurement. A better estimation of the rainfall infiltrations on the volcano flanks would greatly help to better estimate the fluid pressure changes at depth and thus to have a better synthetic model that accounts for velocity changes produced by fluid pressure changes. In the same way, an improved fluid-diffusion model with a nonlinear depth dependence of hydraulic and elastic parameters would be desirable to better model seismic velocity change associated to rainfall. In the case where the timing of the investigated perturbations are unknown using the longest time series available to estimate the transfer function seems to be a reasonable approach as long as it exists a correlation between fluid pressure and seismic velocity changes. Finally, reliable measurements of slight velocity changes coupled with hydrological can also be used to better constrain hydrological parameters such as the hydraulic diffusivity and to validate hydrological models.

Acknowledgments

Seismological data used in this study were acquired by the Institut de Physique du Globe de Paris, Observatoire Volcanologique du Piton de la Fournaise (IPGP/OVPF) and the Institut des Sciences de la Terre (ISTerre) in the framework of ANR-08-RISK-011/UnderVolc project. Several seismic stations belong to the French transportable seismic network, Sismob (INSU-CNRS). Data are available from IPGP (http://centrededonnees.ipgp.fr/index.php?&lang=EN). We are grateful to Meteo France/La Réunion for providing meteorological data. We thank I. Slezak and A. Roques for their useful comments on data processing.

The Editor thanks Yosuki Aoki and an anonymous reviewer for their assistance in evaluating this paper.

References

Brenguier, F., et al. (2008a), Towards forecasting volcanic eruptions using seismic noise, *Nat. Geosci.*, *1*(2), 126–130, doi:10.1038/ngeo104.

Brenguier, F., M. Campillo, C. Hadziioannou, N. M. Shapiro, R. M. Nadeau, and E. Larose (2008b), Postseismic relaxation along the San Andreas Fault at Parkfield from continuous seismological observations, *Science*, *321*(1478), 1478–1481, doi:10.1126/science.1160943.

Brenguier, F., D. Clarke, Y. Aoki, N. M. Shapiro, M. Campillo, and V. Ferrazzini (2011), Monitoring volcanoes using seismic noise correlations, *C. R. Geosci.*, *343*(8–9), 633–638, doi:10.1016/j.crte.2010.12.010.

Brenguier, F., et al. (2012), First results from the UnderVolc high resolution seismic and GPS network deployed on Piton de la Fournaise volcano, *Seismol. Res. Lett.*, *83*(1), 97–102, doi:10.1785/gssrl.83.1.97.

Cappa, F., Y. Guglielmi, S. Viseur, and S. Garambois (2014), Deep fluids can facilitate rupture of slow-moving giant landslides as a result of stress transfer and frictional weakening, *Geophys. Res. Lett.*, *41*, 61–66, doi:10.1002/2013GL058566.

Chen, L., and P. Talwani (2001), Mechanism of initial seismicity following impoundment of the Monticello Reservoir, South Carolina, *Bull. Seismol. Soc. Am.*, *91*, 1582–1594.

Clarke, D., L. Zaccarelli, N. M. Shapiro, and F. Brenguier (2011), Assessment of resolution and accuracy of the Moving Window Cross Spectral technique for monitoring crustal temporal variations using ambient seismic noise, *Geophys. J. Int.*, *186*(2), 867–882, doi:10.1111/j.1365-246X.2011.05074.x.

Costain, J. K., and G. A. Bollinger (2010), Review: Research results in hydroseismicity from 1987 to 2009, *Bull. Seismol. Soc. Am.*, *100*, 1841–1858, doi:10.1785/0120090288.

Derode, B., Y. Guglielmi, L. De Barros, and F. Cappa (2015), Seismic responses to fluid pressure perturbations in a slipping fault, *Geophys. Res. Lett.*, *42*, 3197–3203, doi:10.1002/2015GL063671.

Fischer, T., S. Hainzl, L. Eisner, S. A. Shapiro, and J. Le Calvez (2008), Microseismic signatures of hydraulic fracture growth in sediment formations: Observations and modeling, *J. Geophys. Res.*, *113*, B02307, doi:10.1029/2007JB005070.

Fontaine, F. J., M. Rabinowicz, J. Boulègue, and L. Jouniaux (2002), Constraints on hydrothermal processes on basaltic edifices: Inferences on the conditions leading to hydrovolcanic eruptions at Piton de la Fournaise, Réunion, Island, Indian Ocean, *Earth Planet. Sci. Lett.*, *200*(2002), 1–14.

Froment, B., M. Campillo, J. H. Chen, and Q. Y. Liu (2013), Deformation at depth associated with the 12 May 2008 M_w 7.9 Wenchuan earthquake from seismic ambient noise monitoring, *Geophys. Res. Lett.*, *40*, 78–82, doi:10.1029/2012GL053995.

Gassenmeier, M., C. Sens-Schönfelder, M. Delatre, and M. Korn (2015), Monitoring of environmental influences on seismic velocity at the geological storage site for CO_2 in Ketzin (Germany) with ambient seismic noise, *Geophys. J. Int.*, *200*(1), 524–533.

Hainzl, S., T. Kraft, J. Wassermann, and H. Igel (2006), Evidence for rain-triggered earthquake activity, *Geophys. Res. Lett.*, *33*, L19303, doi:10.1029/2006GL027642.

Hainzl, S., O. Zakharova, and D. Marsan (2013), Impact of aseismic transients on the estimation of aftershock productivity parameters, *Bull. Seismol. Soc. Am.*, *103*(3), 1723–1732, doi:10.1785/0120120247.

Helmstetter, A., and S. Garambois (2010), Seismic monitoring of Séchilienne rockslide (French Alps): Analysis of seismic signals and their correlation with rainfalls, *J. Geophys. Res.*, *115*, F03016, doi:10.1029/2009JF001532.
Hillers, G., M. Campillo, and K.-F. Ma (2014), Seismic velocity variations at TCDP are controlled by MJO driven precipitation pattern and high fluid discharge properties, *Earth Planet. Sci. Lett.*, *391*, 121–127, doi:10.1016/j.epsl.2014.01.040.
Husen, S., C. Bachmann, and D. Giardini (2007), Locally triggered seismicity in the central Swiss Alps following the large rainfall event of August 2005, *Geophys. J. Int.*, *171*, 1126–1134.
Kraft, T., J. Wassermann, and H. Igel (2006), High-precision relocation and focal mechanism of the 2002 rain-triggered earthquake swarms at Mt. Hochstaufen, SE Germany, *Geophys. J. Int.*, *167*, 1513–1528, doi:10.1111/j.1365-246X.2006.03171.x.
Liu, C., A. T. Linde, and I. S. Sacks (2009), Slow earthquakes triggered by typhoons, *Nature*, *459*, 833–836.
Meier, U., N. M. Shapiro, and F. Brenguier (2010), Detecting seasonal variations in seismic velocities within Los Angeles Basin from correlations of ambient seismic noise, *Geophys. J. Int.*, *181*(2), 985–996, doi:10.1111/j.1365-246X.2010.04550.x.
Mordret, A., D. Rivet, M. Landès, and N. M. Shapiro (2014), 3-D shear-velocity anisotropic model of Piton de la Fournaise volcano (La Réunion Island) from ambient seismic noise, *J. Geophys. Res. Solid Earth*, *120*, 406–427, doi:10.1002/2014JB011654.
Muco, B. (1995), The seasonality of Albanian earthquakes and cross correlation with rainfall, *Phys. Earth Planet. Int.*, *88*, 285–291.
Niu, G.-Y., Z.-L. Yang, R. E. Dickinson, L. E. Gulden, and H. Su (2007), Development of a simple groundwater model for use in climate models and evaluation with gravity recovery and climate experiment data, *J. Geophys. Res.*, *112*, D07103, doi:10.1029/2006JD007522.
Obermann, A., T. Planès, E. Larose, and M. Campillo (2013), Imaging preeruptive and coeruptive structural and mechanical changes of a volcano with ambient seismic noise, *J. Geophys. Res. Solid Earth*, *118*, 6285–6294, doi:10.1002/2013JB010399.
Peltier, A., P. Bachèlery, and T. Staudacher (2009), Magma transport and storage at Piton de La Fournaise (La Réunion) between 1972 and 2007: A review of geophysical and geochemical data, *J. Volcanol. Geotherm. Res.*, *184*(1), 93–108.
Peltier, A., J.-L. Got, N. Villeneuve, P. Boissier, T. Staudacher, V. Ferrazzini, and A. Walpersdorf (2015), Long-term mass transfer at Piton de la Fournaise volcano evidenced by strain distribution derived from GNSS network, *J. Geophys. Res. Solid Earth*, *120*, 1874–1889, doi:10.1002/2014JB011738.
Poupinet, G., W. L. Ellsworth, and J. Frechet (1984), Monitoring velocity variations in the crust using earthquake doublets: An application to the Calaveras Fault, California, *J. Geophys. Res.*, *89*, 5719–5731, doi:10.1029/JB089iB07p05719.
Rivet, D., F. Brenguier, D. Clarke, N. M. Shapiro, and A. Peltier (2014), Long-term dynamics of Piton de la Fournaise volcano from 13 years of seismic velocity change measurements and GPS observations, *J. Geophys. Res. Solid Earth*, *119*, 7654–7666, doi:10.1002/2014JB011307.
Roeloffs, E. A. (1988), Fault stability changes induced beneath a reservoir with cyclic variations in water level, *J. Geophys. Res.*, *93*, 2107–2124, doi:10.1029/JB093iB03p02107.
Roult, G., A. Peltier, B. Taisne, T. Staudacher, V. Ferrazzini, and A. Di Muro (2012), A new comprehensive classification of the Piton de la Fournaise activity spanning the 1985–2010 period. Search and analysis of short-term precursors from a broad-band seismological station, *J. Volcanol. Geotherm. Res.*, *241*, 78–104, doi:10.1016/j.jvolgeores.2012.06.012.
Sens-Schönfelder, C., and U. Wegler (2006), Passive image interferometry and seasonal variations of seismic velocities at Merapi Volcano, Indonesia, *Geophys. Res. Lett.*, *33*, L21302, doi:10.1029/2006GL027797.
Sens-Schönfelder, C., E. Pomponi, and A. Peltier (2014), Dynamics of Piton de la Fournaise volcano observed by passive image interferometry with multiple references, *J. Volcanol. Geotherm. Res.*, *276*, 32–45, doi:10.1016/j.jvolgeores.2014.02.012.
Shapiro, S. A., R. Patzig, E. Rothert, and J. Rindschwentner (2003), Triggering of seismicity by pore-pressure perturbations: Permeability-related signatures of the phenomenon, *Pure Appl. Geophys.*, *160*, 1051–1066.
Skempton, A. W. (1954), The pore pressure coefficients A and B, *Geotechnique*, *4*, 143–147.
Svejdar, V., H. Küchenhoff, L. Fahrmeir, and J. Wassermann (2011), External forcing of earthquake swarms at Alpine regions: Example from a seismic meteorological network at Mt. Hochstaufen SE-Bavaria, *Non. Proc. Geophys.*, *18*, 849–860, doi:10.5194/npg-18-849-2011.
Talwani, P. (1997), On the nature of reservoir-induced seismicity, *Pure Appl. Geophys.*, *150*(3–4), 473–492, doi:10.1007/s000240050089.
Talwani, P., L. Chen, and K. Gahalaut (2007), Seismogenic permeability, k_s, *J. Geophys. Res.*, *112*, B07309, doi:10.1029/2006JB004665.
Tsai, V. C. (2011), A model for seasonal changes in GPS positions and seismic wave speeds due to thermoelastic and hydrologic variations, *J. Geophys. Res.*, *116*, B04404, doi:10.1029/2010JB008156.
Zoback, M. D., and H.-P. Harjes (1997), Injection-induced earthquakes and crustal stress at 9 km depth at the KTB deep drilling site, Germany, *J. Geophys. Res.*, *102*, 18,477–18,492, doi:10.1029/96JB02814.